Arab Gulf Journal of Scientific Research, 27 (3): 103- 113 (2009)

Research Paper Ref. No 2495

# Detection and Characterization of Strokes on MRI Brain Images

# كشف و تمييز جلطة المخ فى صور الرنين المغناطيسى الدماغية

*Yazid Cherfa [1], Assia Cherfas [1], and Assia Jaillard [2]*

**يزيد شرفة، اسيا شرفة، وآسيا جايار**

*[1] Electronics Department, Blida's University, P O Box 270, Algeria*

*E-Mail: cherfa_yazid@yahoo.fr & assia_bz@yahoo.fr*

*[2] Neurological Department, Grenoble's Hospital, France*

*E-Mail: Assia.Jaillard@ujf-grenoble.fr*

**Abstract:** In this paper, we present a semi-automatic method for extracting stroke lesions from 2D MRI brain images using edge and region cooperation. Cooperative segmentation is applied after an appropriate image pre-processing using an improvement of the image quality and skull stripping. This segmentation is evaluated thereafter by a comparison to a reference image. To extract and characterize lesions, we apply our method to several MRI images from different subjects who experienced cerebral vascular attacks (strokes). We compare our results with those obtained through manual measurements conducted by neurologists. We apply the results to reconstruct and visualise 3D strokes in the brain.

**Keywords**: *Magnetic resonance image, anisotropic filtering, brain segmentation, stroke, characterization.*

**المستخلص:** في هذه الدراسة، نعرض طريقة شبه أوتوماتيكية لاستخراج المنطقة المصابة نتيجة جلطة دماغية، و ذلك باستعمال صور دماغية للرنين المغناطيسي ذات البعدين. نتحصل على هذا بتطبيق عملية مشتركة بين عمليتي تجزئة المناطق و تجزئة الحدود. بعد عملية نزع المخ من الدماغ و تحسين نوعية الصور لاستخراج المنطقة المصابة بعد تجزئتها نقوم بإجراء حسابات هندسية لتمييز الداء. تطبق هذه الطريقة لعدة صور و تقارن النتائج مع تلك المتحصل عليها يدويا من طرف أخصائيين في الطب. تستعمل صور الجلطة ذات البعدين لبناء صورة ذات أبعاد ثلاثية للجلطة داخل الدماغ. يمكن هذا العمل في الاعانة على تشخيص الداء وفي تسهيل متابعة تطوره مع الوقت، كما يعين أثناء إجراء العمليات الجراحية.

**كلمات مدخلية :** *صور الرنين المغناطيسي للدماغ، الترشيح المتباين، تجزئة الدماغ، السكتة الدماغية، تمييز الخصائص.*

## INTRODUCTION

The brain MRI is an image processing technique used to study the evolution of brain pathologies such as Alzheimer's disease and cerebral vascular accidents (strokes). The timely detection and characterisation of cerebral structures or lesions (e.g., ischemic lesions) are key diagnosis parameters. Image segmentation is one important phase in processing MRI brain images. Segmentation and its application to MRI brain images is still an open and challenging issue (Darbane, *et al*. 1997; Cherfa and Kabir, 1999). It has recently been subject to intensive research efforts (Martel, *et al*. 1999; Pham, *et al*. 1999; Hojjatoleslami and Kruggel, 2001; Yu, *et al*. 2002; Cherfa, *et al*. 2004; Cherfa and All, 2007). Segmentation is challenged by two

important factors: brain complexity and the use of segmentation results by different images.

Physicians are generally interested in finding consistent and reliable approximations of lesion volume from MRI images to evaluate therapies for ischemic stroke patients (Stein, *et al*. 2001). Stroke patient are traditionally assessed through manual segmentation; such segmentation consists of a manual tracing of the stroke regions on all contiguous slices in which the lesion was judged to be present. The tracing is performed by an operator (expert) by pointing and clicking using a mouse-controlled cursor. A simple program connects consecutive points with lines. The lesion region is defined by a closed contour, and the program labels every voxel of the enclosed volume and computes the elementary surface. The volume size is computed by adding the elementary surfaces of all slices.

While manual segmentation is generally considered to be accurate, it is however time consuming and subject to manual variation. Besides, it relies on subjective judgments. This raises the possibility that different observers may reach various conclusions about the presence or absence of affected tissue. To make things even worse, the same observer may reach different conclusions on various occasions ( Fiez, *et al*. 2000).

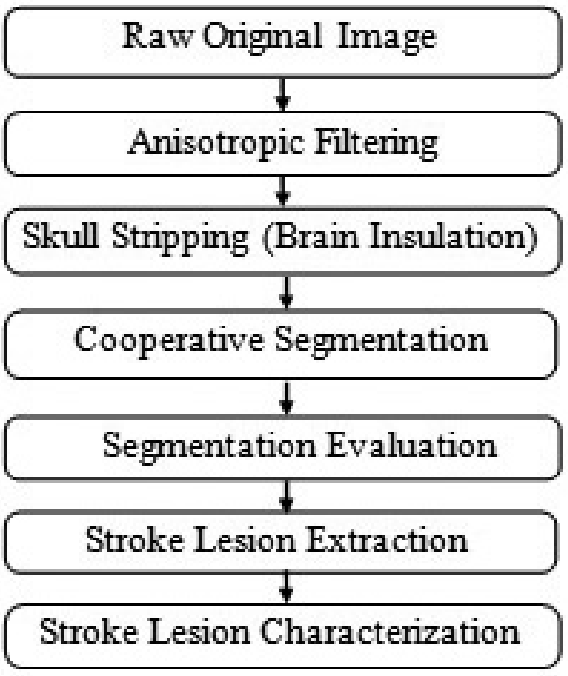


**Fig. 1.** Bloc diagram of the system.

To deal with the aforementioned issues, we propose a semi-automatic method for extracting stroke lesions from 2D MRI brain images. The proposed method segments the stroke lesions that have been localised by a physician and computes geometric features such as the volume, centre of gravity, and shape. In our work, we are interested in preprocessing and segmenting MRI images. MRI images are usually corrupted with different kinds of artefacts including noise, bias that results from the field inhomogeneities, inaccuracies due to patients' movements, and the partial volume effect (Shattuck, *etal*. 2001). The main components of our method are summarised in (Figure 1). The purpose of the first operation is to improve the image quality using a suitable preprocessing before the segmentation step. This is followed by a skull stripping (brain insulation) to avoid segmentation errors. The most important part of our method is segmentation. Segmentation combines edge detection and region extraction. It is evaluated by a comparison to a reference image. The advantages of this approach are discussed by comparing our results with the ones obtained via manual measurements conducted by neurologists.

## PREPROCESSING

Preprocessing in image analysis is compulsory, particularly the filtering and the contrast stretching. The segmentation results are closely related to this first step. Indeed, these some operations will allow us to obtain the best possible images that are a very good representation of the actual images, with a high degree of accuracy and reliability.

### Anisotropic Filtering by PDEs

MR images are strongly corrupted by noise generated by the acquisition system. In order to improve the image quality, we use the technique of anisotropic filtering which allows us to apply a simultaneous filtering and contrast stretching. Anisotropic diffusion is shown to be an energy-dissipating process that seeks the minimum of the energy functional. This kind of filtering belongs to the larger family of Edge Preserving Smoothing Filtering (EPSF) (Gerig, *et al*. 1992) and (Schiess, 2003). These filters preserve the edges of the

objects while filtering the homogeneous zones. This filtering is based on the anisotropic equation of diffusion (1):

$$\frac{\partial I}{\partial t} = div\left[c(f,t).\nabla I\right] \quad (1)$$

where c ($f$, $t$) depends generally on the derivative modulus of $f$, it reaches a maximum when the derivative is equal to zero and it decreases when the gradient increases.

***Second Order PDEs*** (Gallo, *et al*. 1996; You and Kaveh, 2000; Rajan and Kaimal, 2006)

Perona and Malik choose equations (2) or (3) according to the expected result, this could be an edge detection or a region extraction.

$$c(f,t) = \exp\left(-\frac{\left|\nabla f\right|^2}{k^2}\right) \quad (2)$$

$$c(f,t) = \left[1+\left[\frac{\left|\nabla f\right|}{k}\right]^{1+\alpha}\right]^{-1} \quad (3)$$

where $k$ is the diffusion coefficient; it is proportional to a gradient and characterises the amplitude of the gradients that control a strong diffusion:

- If $\nabla f \approx$ k, the diffusion is strong.
- If $\nabla f <<$ k, the diffusion is very weak because the region is regarded as already smooth.
- If $\nabla f >> k$, the diffusion is not carried out because it considered that there is already an edge which has to be preserved by the diffusion.

This iterative filtering operation delivers a simplified image at each iteration; it therefore belongs to the range of multi scale filters. In order to apply this filter, we must choose an appropriate $k$ and the total number of iterations that have to be executed. This number has been fixed to 3 iterations as proposed in (Gerig, *et al*. 1992). The $k$ coefficient influences strongly the smoothing result of a region. In fact, the filter does the smoothing when the region is corrupted and the gradient is close to $k$. We have fixed k to 14, as this leads to edge preservation and smoothing of homogeneous regions.

The second order anisotropic diffusion is designed such that smooth areas are diffused faster than less smooth ones, blocky effects will appear in the early stage of diffusion, even though all the blocks will finally merge to form a level image. When there is backward diffusion, however, any step image (piecewise level image) 1 is a global minimum of the energy functional, so blocks will appear in the early stage of the diffusion and will remain as such. The fourth-order PDEs is a technique to avoid blocky effects while achieving good trade off between noise removal and edge preservation.

***Fourth Order PD Es*** (You and Kaveh, 2000; Lysaker, *et al*. 2003; Rajan and Kaimal, 2006)

There are good reasons to consider fourth order equations:

fourth order linear diffusion damps oscillations at high frequencies much faster than second order diffusion;

there is the possibility of having schemes that include effects of curvature in the dynamics, thus creating a richer set of functional behaviours;

We can show that a planar image is a global minimum of the cost functional E(I) .

$$E(I) = \int_{\Omega} f(\left|\nabla^2 I\right|)d\Omega \quad (2)$$

The Euler equation which result of You and Kaveh (Darbane, *et al*. 1997) work may be solved through the following gradient descent procedure:

$$\frac{\partial I}{\partial t} = -\nabla^2\left[f'(\left|\nabla^2 I\right|)\frac{\nabla^2 I}{\left|\nabla^2 I\right|}\right] = -\nabla^2\left[c(\left|\nabla^2 I\right|)\nabla^2 I\right. \quad (3)$$

with the observed image as the initial condition. The solution is arrived when t→∞, but the time evolution may be stopped earlier to achieve an optimal trade off between noise removal and edge preservation. Also, it should be mentioned that the contrast stretching is fulfilled, resulting from the anisotropic diffusion principle.

**Skull Stripping (Brain Insulation)**

The goal of this phase is to extract the brain from the acquired image; this will allow us to simplify the segmentation and the characterisation of the stroke (Schiess, 2003). The problems in this operation are the existence of noise on the image

and the non-uniformity of the grey levels of the image background. Several methods based on the use of deformable models and mathematical morphology has been proposed. Our original method can be divided in six steps:

***Binarisation***

Fixing an adequate value of a threshold *S*, the background noise contained in the original image is decreased as shown in (Figure 2-B). This is achieved using the following test:

$$I_B(x,y)=\begin{cases}0 & \text{if } I_{orig}(x,y)<S\\ 255 & \text{if } I_{orig}(x,y)>S\end{cases} \quad (4)$$

(x,y) the coordinates of courant pixel.

***Filtering***

The resulting image is filtering using a mean filter; this will decrease the noise present on the input image. This is illustrated in (Figure 2-C).

***Dilation***

This operation consists of eliminating all remaining black spots on the white surface of the image. These spots are covered by the dilation of the white parts. This process is carried out by moving a square ($N$ x $N$) mask on our image and applying the logical OR operator on each of the ($N^2$ - 1) neighbouring pixels (Figure 2-D). N x N the size of rhombus structuring element.

$$I_D(x,y)=\begin{cases}I_f(x,y)\\ 0\end{cases} \quad (5)$$

***Erosion***

On the other side, the process of erosion consists on applying the logical *AND* operator on the ($N^2$ - 1) neighbouring pixels. After this operation, all white spots of the image disappear.

$$I_E(x,y)=\begin{cases}I_D(x,y) & \text{If the AND operation gives 1}\\ 0 & \text{Otherwise}\end{cases} \quad (6)$$

***Filling the Holes***

The remaining holes in the image are filled using the following procedures:

- *Labelling:* it consists to assign the same label to the black marked pixels that belong to the same connected component.
- *Centre of gravity computation:* of each component of the labelled image.
- *Filling the holes:* This step is carried out by checking, for each connected "child" component, whether its centre of gravity belongs to another connected "parent" component whose number of pixels is higher than that of the "child". If this is the case, the grey level of the "child" will be replaced by that of the "parent" (Figure 2-F).

***Image Masking***

The binary image or the obtained mask is combined with the original image using a logical operator. To extract the cortex, we apply the *OR* operator as shown in (Figure 2-H), otherwise we use the *AND* operator to extract the brain as shown in (Figure 2-G).

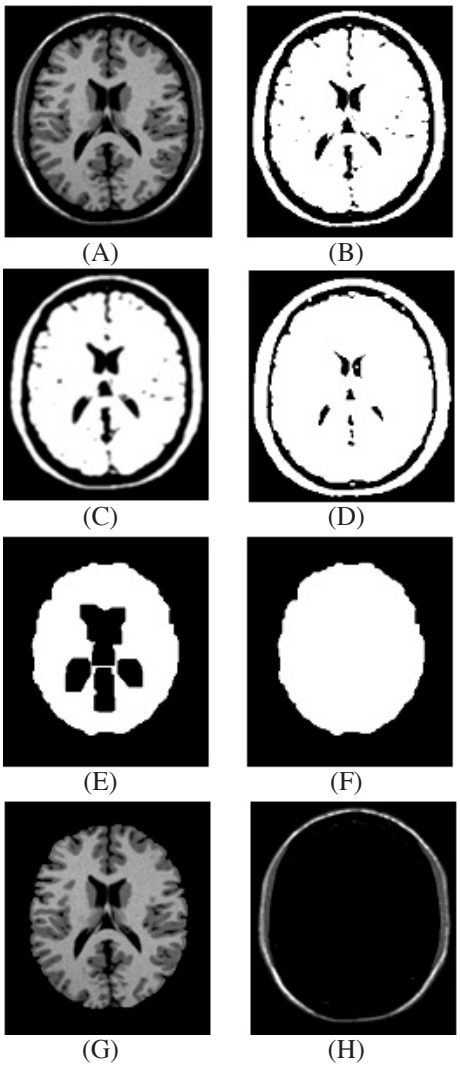


**Fig. 2 (A-H)** Brain extraction steps.

## COOPERATIVE SEGMENTATION

This cooperation is based on the edge-region duality (Cherfa and All, 2007), and summarised by the bloc diagram as shown in (Figure 3).

### Edge Detection

This is carried out using the Deriche operator (Canny, 1983; Deriche, 1987) . In addition to its robustness, the latter has the advantage of giving the possibility to change the parameters according to our needs. This operation uses an optimal infinite impulse response filter as expressed by the following equation:

$$f(x) = ce^{-\alpha|x|} \sin wx \; ; x \in [-\infty, +\infty] \qquad (7)$$

with σ the filtering intensity. This method can be divided into the following steps:

- This filter is applied along the x and y directions;
- Derivatives computation with respect to x and y;
- Norm image gradient computation;
- Local maximum extraction;
- Thresholding by hysteresis (Sb and Sh);
- Edge image creation.

### Small Edges Elimination

In this step, we use a thresholding to eliminate the false edges, due to the eventual presence of disturbed or textured regions. These edges are rather shorts and without semantic interpretation. The used threshold depends on a priori information about the image to be analysed.

### Region Growing

The isotropic growth used (Hojjatoleslami and Kruggel, 2001; Cherfa, *et al*. 2004) is conditioned by the edges, it must also obey to a double criterion; the growing procedure is stopped if:

- The homogeneity criterion is not fulfilled;
- The analysed pixel belongs to an edge chain.

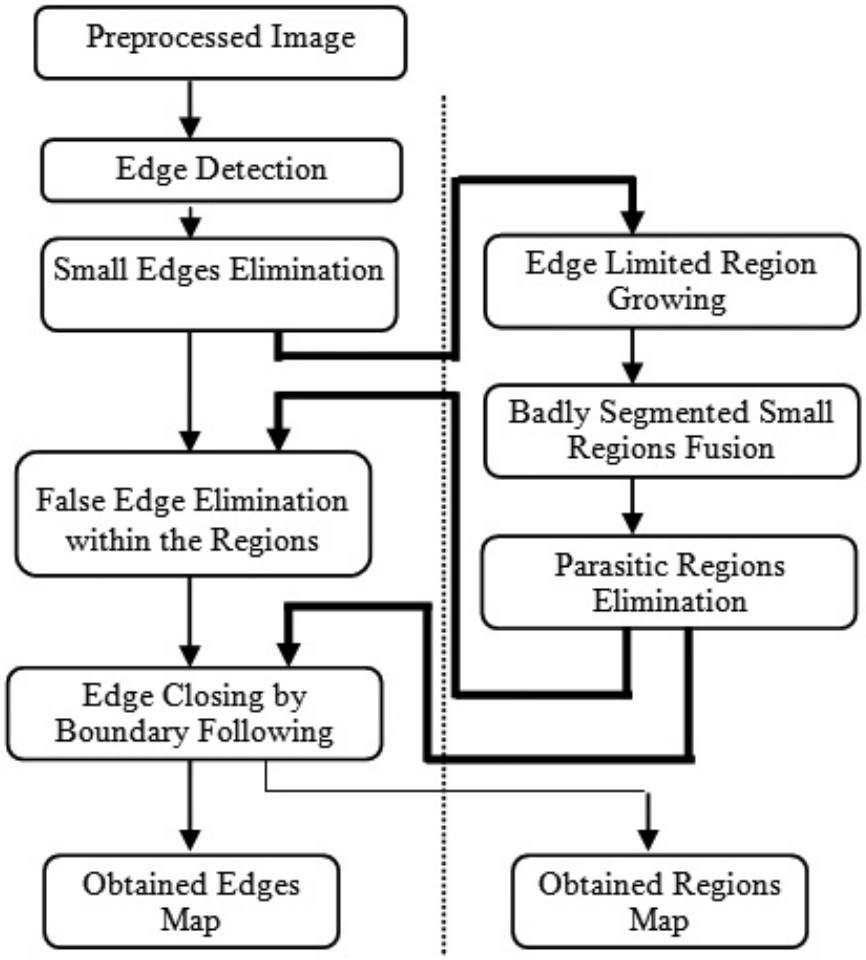


**Fig. 3.** Cooperation block diagram.

The homogeneity criterion used is the grey level difference. The following consists in placing the seeds at the places within the zones of interest by an expert. The isotropic growth is carried out by sequentially testing the seed neighbouring pixels without giving privilege to any direction. When the seed *Gr* is positioned, their neighboured pixels was chosen in the unitary grid (Figure 4) on the 8-connexity, in the following order:

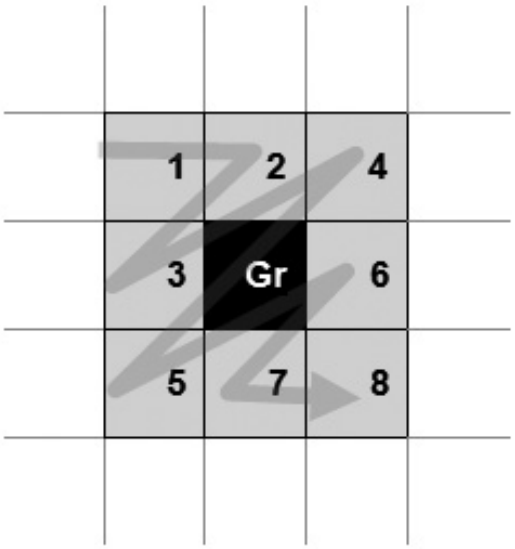


**Fig. 4.** The seed Gr and his 08 neighbours in priority order.

**Badly Segmented Small Regions Fusion**

Unwanted small regions are generated because of the edge constraint and the segmentation parameters choices. To correct this problem, these will be merged with the parent region. This method is based on a triple test: on their size, on the grey level comparison with that of the parent region, and on the fact that they coincide with edge pixels. These small regions must be merged with adjacent region having the closest grey level as shown in (Figure 5).

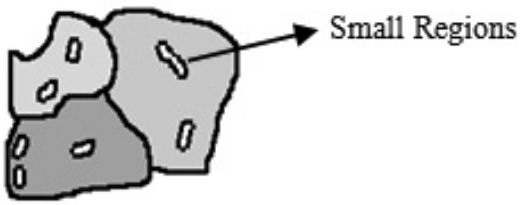


**Fig. 5.** Example of region fusion.

**Removing the Parasitic Regions**

After the growing operation, we sometimes have the apparition of small parasitic areas between two adjacent regions. Again, in this case, we proceed as above, i. e. these areas are merged with the closest regions that have the nearest level of grey.

**False Edge Elimination**

In addition to the above operation, we must take into account the existence of eventual false edges within homogeneous regions. If this is the case, they must be removed.

**Edge Closing**

Segmentation produces some edges that are rarely closed. In order to complete the closing of all the edges, we use the data from the region map that will give us the possibility to follow the closest boundary in terms of the Euclidian distance as shown in (Figure 6).

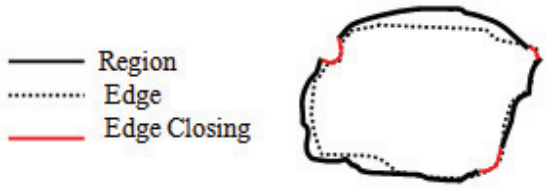


**Fig. 6.** Example of edge closing.

The overall result of segmentation is therefore the availability of two compatible maps, edge and region maps.

## SEGMENTATION EVALUATION

To validate the results obtained by our method, an evaluation of the segmentation will be carried out. Several methods have been proposed in the literature (Zhang, 1996). We have chosen the Pratt method; it's used to assess performance of edge segmentation techniques. This approach is based on the use of a reference image as a ground truth. This allows us to quantify the performance of our segmentation compared with that obtained from a manual segmentation. Let us consider an edge map A and a reference map I, we define the Pratt index by the following expression:

$$F(I,A)=\frac{1}{\max\left(I_A,I_i\right)}\times\sum_{i=1}^{I_A}\frac{1}{1+\alpha d^2} \qquad (8)$$

where *d(i)* is the distance between the edge pixel *i* of the map A and the closest edge pixel of the reference map I, $I_A$ and the $I_i$ are the number of the edge pixels of the A and I maps respectively. α is a coefficient used to have $0 \leq F \leq 1$.

A good segmentation is obtained (comparable to that of the reference image) if *F* is close to 1. The ground truth image used in our application is an MR image manually segmented by a medical expert as shown in ( Figure 7).

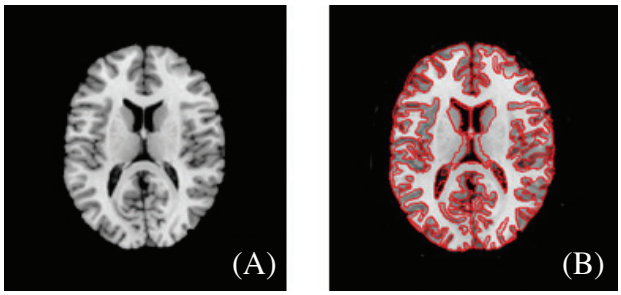


**Fig. 7 (A-B)** Original image and reference segmented image.

### The Anisotropic Filtering Effect

The following experiment will show the influence of the anisotropic filtering on the segmentation quality. We use the cooperative segmentation with the same parameters applied on both the preprocessed image and the unprocessed image as shown in Figure 8.Then we use the Pratt index F to evaluate the effect of anisotropic filtering as shown in (Table 1).

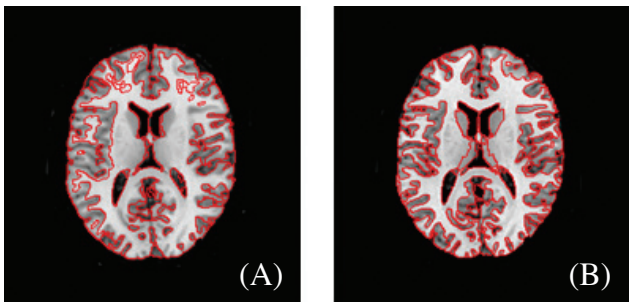


**Fig. 8 (A-B)** The processed segmented image, (b) Anisotropic filtering segmented image.

**Table 1.** Pratt Index for various segmentations

| Segmentation | F Index |
|---|---|
| **Unprocessed Segmentation** | 66,75% |
| **Anisotropic Filtered Segmentation** | 71,13% |

From Table (1), we can clearly see that using a suitable preprocessing improves the segmentation quality.

### The Cooperation Effect

In this experiment, we will show the effect of cooperation on the segmentation results. We apply the Deriche operator and our cooperative approach to the same reference image using the same preprocessing as shown in Figure (9) and Table (2).

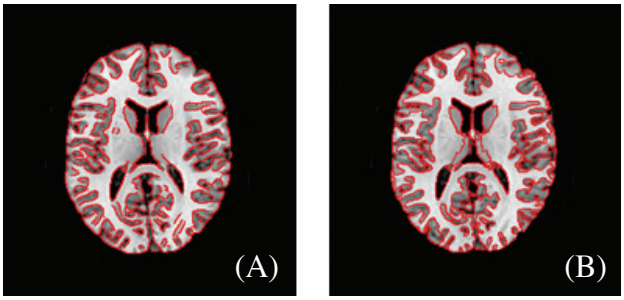


**Fig. 9 (A-B)** Deriche segmented preprocessed image, (b) Our approach segmented preprocessed image.

**Table 2.** Cooperative effect.

| Segmentation | F Index |
|---|---|
| **Deriche Operator** | 64,27% |
| **Our Cooperative Approach** | 71,13% |

The cooperation effect gives also an improvement in the segmentation results. Using the Deriche edge extraction as followed by an application of the cooperative approach improves the segmentation quality.

## APPLICATIONS: EXTRACTION AND CHARACTERIZATION OF STROKE LESIONS IN MR BRAIN DAMAGE

Our system will be used to characterise the stroke region in the brain of an affected patient. Because the procedure of this characterisation is not automated, the user must choose the region to be segmented by manually choosing the growing seeds positions on the stroke lesion. This procedure allows to extract the lesion and to characterise it

by some geometrical measurements. We have used three acquisition sequences: Diffusion images, Flair images and T2-Weighted images as shown in Figure 10 (A-C). The MR Images are acquired in 3D and are converted in 2D slices (18 to 20 in our case). For each MR image sequence, we used one slice in order to study the evolution of two geometrical characteristics: surface and distance between centres of gravity of the brain and the lesion.

**Preprocessing**

In the first step, we apply the anisotropic filtering followed by an extraction of the brain from all images as shown in Figure 10, d, e, and f. For the second order anisotropic filter, we have used the following parameters:

- The number of iterations is fixed to 3;
- The *k* coefficient influences is fixed to 14.

For the fourth order anisotropic filter, we have used the following parameters:

- The number of iterations is fixed to 3;
- The *k* coefficient is fixed to 0,5;
- T=1; ΔT=0,9.

**Segmentation and Characterization**

The cooperative segmentation described previously will be applied to extract the stroke lesion. We have used the following parameters:

- Deriche procedure: σ = 1; Sh=25; Sb=15;
- Small Edges Elimination threshold: 5;

The stroke lesion will be characterised using the calculation of it surface, its centre of gravity and that of the brain.

***Surface Calculation***

This calculation is carried out by counting the number of pixels of the extracted stroke image.

***Centre of Gravity Calculation***

The centre of gravity coordinates are calculated in the following way:

$$X = \frac{\sum_{i=0}^{255} m_i x_i}{\sum_{i=0}^{255} m_i}; \quad Y = \frac{\sum_{i=0}^{255} m_i y_i}{\sum_{i=0}^{255} m_i} \tag{9}$$

where xi and yi are the coordinates of the region perimeter points and mi their grey level. The coordinates of the two centres of gravity (brain and lesion) allow us to calculate the distance between them and informs us about the stroke position. These measurements will be compared with those obtained from medical experts.

***Stroke Medical Expertise***

In order to validate this semi-automatic characterisation, a medical expertise is essential. To achieve this, we have developed software that will allow the physicians to delimit the lesion edges on MR brain images. The obtained region is characterised by a similar routine to that of the semi-automatic method. This is illustrated by Figure 10 (A-L).

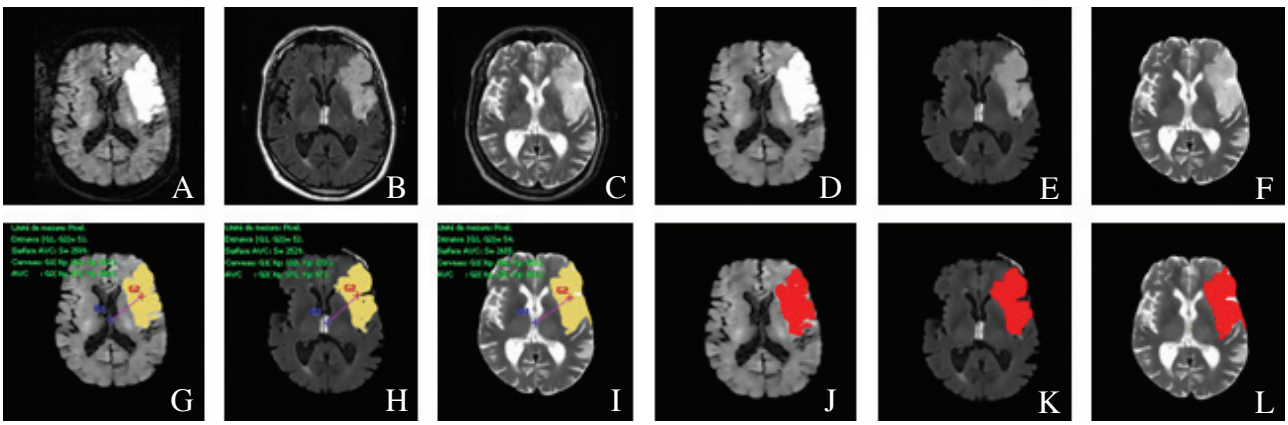


**Fig. 10** (A-L) Multi-sequence MR Images (A): Diffusion; (B): Flair; (C): T2-weighted; (D), (E), (F): Preprocessed images; (G), (H), (I): Segmented and characterized images by our method; (J), (K), (L): Manually expertised and characterized images.

## RESULTS AND DISCUSSION

In Tables ( 3) and ( 4), we have gathered all the obtained results.

Analysing the above results, the following observations can be made:

- The cooperative segmentation allows an efficient stroke lesion extraction.
- A comparison of the surface of the stroke using both methods shows that the results are very close (2 - 4% error).
- The two methods give very similar values of the stroke centre of gravity.
- The cooperative segmentation simplifies the extraction and the characterisation of the stroke from MR Images. This can be viewed as a minor contribution for stroke diagnosis.
- In addition to its simplicity, the overall procedure is computed in less than 5 seconds.

**Table 3.** Comparison between stroke surfaces extracted by our method and a medical expertise.

| Method | Surface Coop | Surface Exp | Error |
|---|---|---|---|
| **Diffusion** | 2589 | 2482 | 4,1% |
| **Flair** | 2529 | 2590 | 2,4% |
| **T2** | 2655 | 2595 | 2,3% |

**Table 4.** Comparison between the co-ordinates of stroke gravity centres extracted by the two methods.

| Method | Co-ordinates (x, y) of GC segmented stroke | Co-ordinates (x, y) of GC expertised stroke |
|---|---|---|
| **Diffusion** | (173,100) | (172,99) |
| **Flair** | (171,97) | (170,96) |
| **T2** | (173,101) | (172,100) |

### 3D Stroke reconstruction

We visualise the stroke in the brain with a 3D reconstruction procedure in order to assist the surgeon in the chirurgical operations. We have used 18 MRI brain images (Figure 11) segmented by our method where the strokes are completely extracted. The extracted strokes are then reconstructed in 3D image (Figure 12).

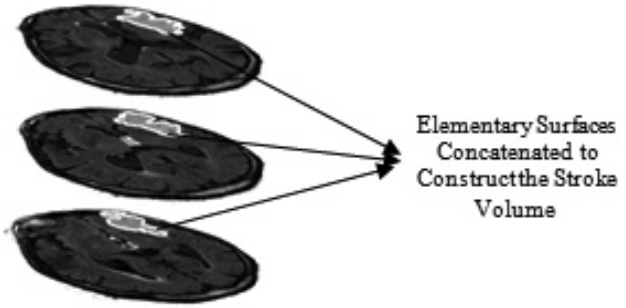


**Fig. 11.** Segmentation slice by slice to construct the stroke volume.

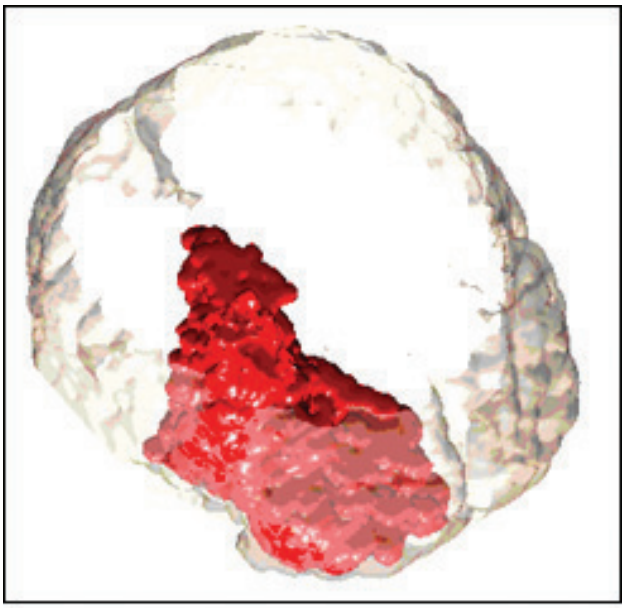

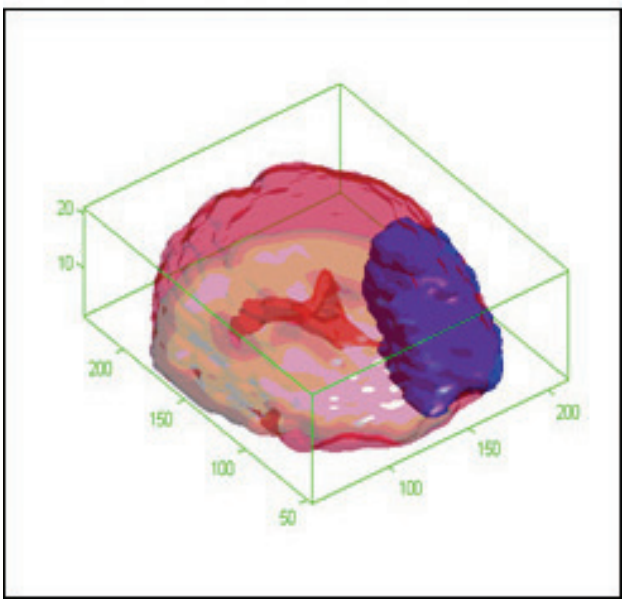


**Fig. 12.** 3D Reconstruction of the brain with stroke lesion.

## CONCLUSION

We have introduced a simplified method that can be used to improve the different steps results applied to medical images. Our method uses adequate pre-processing followed by an edge-region cooperative segmentation technique to extract stroke lesions. The segmentation allows the characterisation of stroke affected regions; this will give the possibility to study the time evolution of some particular attributes. From a medical point of view, this tool improves the harnessing of the information contained in medical images by a better characterisation of the affected regions and cerebral plasticity. It can help and assist physicians in the diagnosis of stroke lesions. This provides information that is clinically relevant to the prognosis of the disease. This system is being applied to study the time evolution of the lesion for 50 stroke patients.

## ACKNOWLEDGEMENTS

This work was supported by a special cooperation programs CMEP 03MDU588 between the Saad Dahlab University of Blida (Algeria) and the Joseph Fourier University of Grenoble (France). Many thanks to a neurology department of Grenoble hospital that provides us with the stroke MR Images, and to Mr Michel Dojat from GIN in Grenoble and Mrs Catherine Garbay from CLIPS Laboratory in Grenoble to their contribution. The present paper was translated with the help of Dr B.Kazed.

## REFERENCES

**Canny, J.F** (1983) *Finding Edges and Lines in Images*. *Technical report* AI-TR-720. MIT Artificial Intel. Lab, Cambridge, MA.

**Cherfa, Y**, and **All** (2007) Segmentation of magnetic resonance brain images using edge and region cooperation: characterization of stroke lesions *International*. *Arab Journal of Information Technology* **4 (3):** 281-288.

**Cherfa, Y**, and **Kabir, Y** (1999) *X-Rays Image Segmentation, IEEE-EURASIP Workshop on linear Signal and Image Processing*. Antalya, Turkey.

**Cherfa, Y, Jaillard, A, Cherfa, A, Kabir, Y, Kassous, S, Gaceb, D, Garbay, C,** and **Dojat, M**, (2004) Segmentation coopératived'images RMN cérébrales. *In*: *Proceedings of JETIM'2004*. Blida, Algérie, pp. 35-41.

**Darbane, S, Drai, R, Cherfa, Y,** and **Kabir, Y** (1997) Detection of welding defects in X-ray images by image segmentation. *Annales de Chimie - Science des Matériaux* **22 (143):** 133-141.

**Deriche, R** (1987) Using canny's criteria to derive a recursive implemented optimal edge detector. *International Journal of Computer Vision*. **1 (10):** 167-187.

**Fiez, J, Damasio, H,** and **Grabowski, G** (2000) Lesion segmentation and manual warping to a reference brain: intra- and interobserver reliability. *Human Brain Mapping* **9 (4):** 192-221.

**Gallo, G, Zingale, A,** and **Zingle, R** (1996) Detection of MRI brain contour using nonlinear anisotropic diffusion. *In*: *International Conference of IEEE Engineering in Medicine and Biology Society*, Amsterdam, Netherlands, pp. 1062-1064.

**Gerig, G, Kübler, O, Kikinis, R,** and **Jolesz, FA** (1992) Nonlinear anisotropic filtering of MRI data. *IEEE Transactions on Medical Imaging***11 (2):** 221-232.

**Hojjatoleslami, SA, and Kruggel, F** (2001) Segmentation of large lesions. *IEEE Transactions on Medical Imaging* **20 (7):** 666-669.

**Lysaker, M, Lundervold, A**, and **Tai, XC** (2003) Noise removal using fourth order partial differential equation with applications to medical magnetic resonance images in space and time. *IEEE Transactions on Image Processing* **12 (12):** 1579 – 1590.

**Martel, AL, Allder, SJ, Delay, GS, Morgan, PS**, and **Moody, AR** (1999) Measurement of infarct volume in stroke patients using adaptive segmentation of diffusion weighted MR images. *MICCAI'99 of Computer Science* **1679:** 22-31.

**Pham, DL, Xu, C**, and **Price, J.L** (1999) *A Survey of Current Methods in Medical Segmentation*, *Technical Report JHU/ECE 99-01*. University of Baltimore, USA.

**Rajan, J** .and **Kaimal, MR** (2006) A comparative analysis of fourth order and complex PDEs for noise removal. *In*: *International Journal on Systemics Cybernetics and Informatics*, pp.63 -68.

**Schiess, M,** (2003) *Segmentation d'image anatomique du cerveau chez l'adulte*. Thèse de l'école d'ingénieurs de Genève.

**Shattuck, DW, Sandor-Leahy, SR, Schaper, KA, Rottenberg, DA,** and **Leahy R** (2001) Magnetic resonance image tissus classification using a partial volume model. *NeuroImage* **5 (13):** 856-876.

**Stein, B, Lisin, D, Horowitz, J, Riseman, E**, and **Whitten, G** (2001) Statistical and deformable model approaches to the segmentation of MR imagery and volume estimation of stroke lesions. *In: Proceedings of 4th International Conference on MmEDICAL Image Computing and Computer-Assisted Intervention*. Utrecht, Netherlands, pp.829-836.

**You, YL,** and **Kaveh, M** (2000) Fourth order partial differential equations for noise removal. *IEEE Transactions on Image Processing* **9 (10):** 1723-1730.

**Yu, S, Pham, D, Shen, D,** and **Gerskovits, E** (2002),Automatic segmentation of white matter lesions in T1-weighted brain MR images. *In*: *Proceeding of IEEE International Symposium on Biomedical Imaging*. Washington, pp. 253-256.

**Zhang, YJ** (1996) A survey on evaluation methods for image segmentation *Pattern Recognition* **29:** 1335- 1346.

Ref. No. (2495)
Rec. 09/09/2008
In-revised form: 11/09/2009